CT Assessment of Global and Regional Cardiac Function: State of the Art

Rishi Agrawal and Suhny Abbara

Contents

R. Agrawal · S. Abbara (✉)
Cardiac MRCT Program, Massachusetts General Hospital,
Boston, MA, USA
e-mail: SAbbara@Partners.org

Abstract

Reliable assessment of cardiac function is an important tool for diagnosis and prognosis of multiple cardiac and extracardiac diseases. Echocardiography and MRI are the most commonly used methods to evaluate cardiac function, but can be limited or contraindicated in certain patients. Functional evaluation with CT may play an important role in these patients and in those patients being evaluated for coronary artery disease. Functional imaging requires a retrospectively gated acquisition and special attention must be paid to the contrast injection technique for appropriate analysis. Left and right ventricular analysis is evaluated both quantitatively and qualitatively. Quantitative measurements with CT have shown close correlation with values obtained with CMR. Acute and chronic infarcts and non-ischemic cardiomyopathies can have a characteristic appearance on imaging. Functional and volumetric measurements of the left atrium can be carried out with similar technique for evaluation of patients with mitral disease or atrial fibrillation.

Abbreviations

CMR	Cardiac magnetic resonance
DSCT	Dual-source computed tomography
ED	End diastolic
EF	Ejection fraction
ES	End systolic
LA	Left atrium
LV	Left ventricle
LVEF	Left ventricular ejection fraction
MDCT	Multi-detector computed tomography
PET	Positron emission tomography
RA	Right atrium
RV	Right ventricle
RVEF	Right ventricular ejection fraction
RVOT	Right ventricular outflow tract

1 Introduction

1.1 Value of Functional Information of RV and LV

Reliable assessment of cardiac function is important for diagnosis and prognosis in multiple disease states of both cardiac and non-cardiac origin. For example, left ventricular (LV) ejection fraction is an independent predictor of survival in patients after myocardial infarction (Hammermeister et al. 1979). Additionally, in patients studied after coronary artery surgery, LV ejection fraction was shown to be a more important predictor of survival than the number of coronary arteries bypassed (Mock et al. 1982). Independent examination of LV function is important because the degree of coronary stenosis and LV function is nonlinear; once a certain threshold stenosis is reached, LV function begins to decline precipitously. Conversely, LV dysfunction, even in a regional distribution, does not always predict an underlying coronary lesion. (Juergens and Fischbach 2006) CTA provides the unique ability to evaluate both structure and function with a single test, offering convenience for both patients and clinicians.

Right ventricular (RV) function also carries important prognostic implications in numerous diseases such as acute pulmonary embolism, liver failure, arrhythmogenic right ventricular dysplasia, and congenital heart disease. Reliable and accurate assessment of the RV by CTA can be particularly helpful due to the difficulties in imaging the RV with other modalities. Function and volume measurements of the left atrium also carry prognostic significance. In particular, they are important predictors of recurrence of atrial fibrillation after pulmonary vein isolation or left atrial ablation.

In comparison to coronary artery imaging alone, functional imaging of the heart involves measurement of chamber volumes including both end-systolic volume (ESV) and end-diastolic volume (EDV). Using this information, stroke volume (SV), ejection fraction (EF), and cardiac output (CO) can be calculated. Function is also assessed qualitatively by examining the movement and wall thickening of the myocardium.

1.2 Existing Noninvasive Methods to Quantify Function

There are many noninvasive methods to quantify cardiac function including echocardiography, radionuclide ventriculography (RVG), gated single photon emission computed tomography (SPECT), gated positron emission tomography (PET), and cardiac magnetic resonance imaging (CMR). With improvements in CT technology such as multi detector-row computed tomography (MDCT) and dual source computed tomography (DSCT), CT has played an increasing role in determining cardiac function.

1.2.1 Echocardiography

Transthoracic echocardiography continues to be the most commonly used technique to evaluate cardiac function due to its widespread availability, portability, and cost. Echocardiography has the ability to measure chamber sizes and volumes, to calculate ejection fraction, and to analyze valvular function. Doppler imaging improves quantification by allowing measurement of velocities and pressure gradients through valve planes and orifices. Newer techniques like 3D ultrasound and newer software allow more reliable quantification of ventricular function.

Echocardiography, however, is limited in large patients owing to reduced ultrasound beam penetration. Additionally, evaluation of the right ventricle is limited due to suboptimal acoustic windows. Trans-esophageal echocardiography improves on these limitations but introduces additional risks associated with anesthesia and esophageal injury. Because formulas used to calculate atrial and ventricular volumes use geometric assumptions of cardiac shape, measurements in patients with remodeled cardiac chambers can be inaccurate.

1.2.2 Radionuclide Imaging

Nuclear medicine techniques to quantify cardiac function include RVG, SPECT, and PET. Whereas the purpose of RVG is to quantify left ventricular function, SPECT and PET are performed for evaluation of cardiac perfusion and metabolism. RVG utilizes ^{99m}Tc-labeled erythrocytes to directly image the blood pool and, as such, does not rely on geometric assumptions to quantify ventricular function (de Geus-Oei et al. 2011). A gated image is obtained by combining counts over multiple heartbeats, though first-pass imaging can also be performed. Both SPECT and PET rely on ventricular contour analysis to measure function. The advantage of both SPECT and PET is the additional information that each of these modalities affords. Compared to SPECT, PET offers greater spatial resolution, which may more accurately measure left ventricular function, particularly in patients with a small left ventricular volume (Slart et al. 2004). Functional data obtained with both SPECT (Bavelaar-Croon et al. 2000) and PET (Slart et al. 2004) correlates closely with functional data obtained with CMR.

There are certain limitations associated with each of these modalities. Because RVG image data is combined over multiple heartbeats, its utility can be limited in patients with an irregular rhythm. Gated SPECT is limited by low spatial resolution. Additionally, in patients with prior myocardial infarct, SPECT may show very little or no radiotracer uptake in the corresponding region of the

myocardium, preventing accurate delineation of the endocardial border (Stollfuss et al. 1998). PET suffers from lower temporal resolution than MRI, which may contribute to underestimation of cardiac function. Also, because papillary muscle signal is merged with the myocardial wall in PET, cavity volume is reduced compared to MRI which includes papillary muscle in the ventricular cavity (Slart et al. 2004). All three methods have the disadvantage of using ionizing radiation to generate images.

1.2.3 MRI

Cardiac MRI is now considered the gold standard for the assessment of cardiac function offering both high temporal resolution, allowing accurate imaging of end-systole and end-diastole, and moderately high spatial resolution, permitting accurate delineation of cardiac contours. Many studies have shown CMR to be highly accurate and reproducible (Setser et al. 2000). Imaging can be performed in any imaging plane, though quantitative assessment is usually accomplished in the short-axis plane using Simpson's method. Two-chamber, three-chamber, and four-chamber views can be obtained easily to evaluate regional wall motion abnormalities and valvular function. Detection of delayed myocardial enhancement and the development of a multitude of cardiac-gated pulse sequences have expanded the role of cardiac MRI quite extensively.

Cardiac MRI may be contraindicated in patients with pacemakers and many other metallic implanted devices. Additionally, due to the length of the study and the need to include the chest within the bore of the magnet, cardiac MRI is limited in patients with claustrophobia. The discovery of nephrogenic systemic fibrosis (NSF) in patients with renal failure receiving certain gadolinium-based contrast agents has decreased the use of IV gadolinium-based contrast in patients with renal failure. However, for strictly functional measurements, IV contrast is not needed.

1.3 Indications/Contraindications

Most cardiac CT performed today is done for the purpose of evaluating the coronary arteries rather than for the explicit purpose of measuring right or left ventricular function. Some circumstances call for the use of cardiac CT as the primary tool for determining cardiac function, usually in situations when other imaging modalities such as echocardiography or CMR are limited. For example, it is useful in patients with contraindications to MRI such as claustrophobia or implanted metallic devices. It is also useful in patients whose echocardiography study may be limited due to large body habitus. Additionally, cardiac CT is less operator-dependent compared to echocardiography and can be performed relatively quickly, making it useful in patients who cannot hold

their breath or lay still for prolonged periods of time. Current ACR appropriateness criteria calls for the use of cardiac CT for the evaluation of cardiac function in patients post-myocardial infarction or in patients with heart failure if other methods of noninvasive imaging are inadequate. It is also an accepted modality for evaluation of right ventricular function and for evaluation of the pulmonary veins and left atrium prior to invasive pulmonary vein isolation. There are few contraindications to cardiac CT, the major reason being severe allergy to iodinated contrast. Even patients with mild allergy to iodinated contrast can be pre-treated with steroids and diphenhydramine to reduce the risk of allergic reaction. Patients with renal failure have an increased risk of contrast-induced nephropathy, though this is not an absolute contraindication.

1.4 Drawbacks

1.4.1 Temporal Resolution

One of the main challenges of imaging the heart is to reduce blurring artifact created with cardiac motion. The most important hardware parameter that deals with this challenge is the temporal resolution which is a function of the gantry rotation speed. For the purposes of generating an image, only a half-gantry (i.e. 180°) rotation is needed on traditional single source scanners. Scanners with faster gantry rotation have improved ability to freeze cardiac motion. Because the position of the ventricular wall at end-diastole and end-systole is averaged over the rotation interval, scanners with slower gantry rotation times (i.e. longer rotation interval) have greater potential for overestimation of ESV and underestimation of EDV (Fig. 1). Early attempts at functional cardiac imaging using 4-slice MDCT suffered from poor temporal resolution. To compensate, multi-segment reconstruction algorithms were utilized. Using this method, data from 2 (or more) different heartbeats acquired at the same phase of the cardiac cycle are combined to make an image. Two-segment reconstruction maximally decreases the temporal resolution to one half (e.g. from 210 to 105 ms), however, the degree of reduction is highly dependent on the heart rate and at some heart rates there is no improvement in temporal resolution. This technique is also susceptible to image artifacts if the heart is not in the exact same position during the second heartbeat or if there is significant beat-to-beat variability in heart rate.

Modern-day single source CT scanners have much improved gantry rotation times (down to 270 ms), largely eliminating the need for multi-segment reconstruction. Dual source CT improves on this temporal resolution by adding a second X-ray source and detector, positioned 95° from each other, approximately halving the temporal resolution of a single source system. Currently, the fastest available DSCT
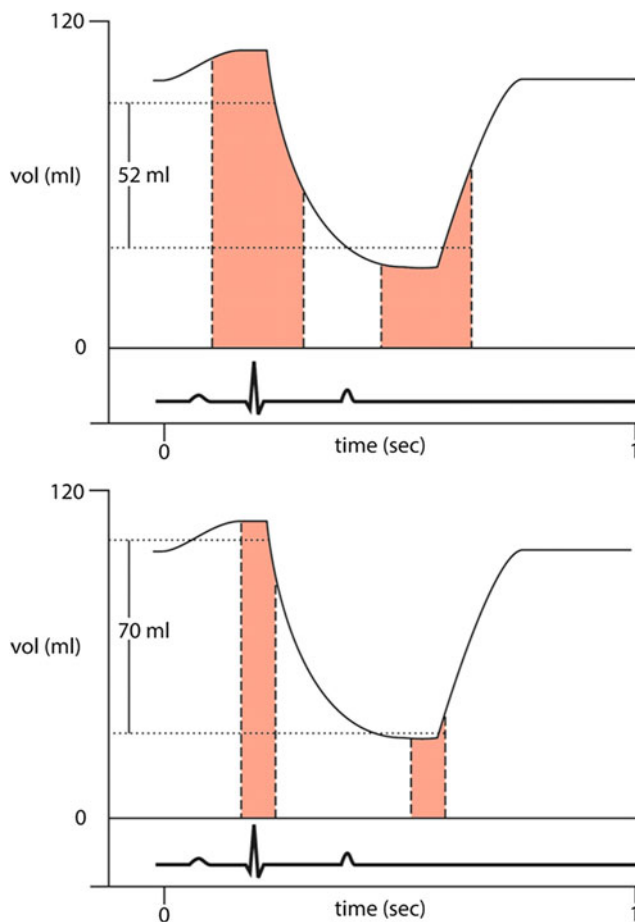
Fig. 1 Effect of temporal resolution on volume measurement. Identical time-volume curves are shown in a patient with a heart rate of 60 bpm. *Red bars* indicate sampling by the scanner. The *top* image represents a scanner with a half-gantry rotation time of 200 ms. The image data is averaged through both end-systole and end-diastole causing over-estimation of the volumes in end-systole and under-estimation of end-diastole. The *bottom* image represents a scanner with a half-gantry rotation time of 100 ms. Because the image is generated over a shorter time frame, end-systole and end-diastole more closely reflect the true values, yielding a higher ejection fraction

can cover a 180° arc of projections in ∼75 ms. In comparison, MRI has a temporal resolution of approximately 30 ms. Despite these limitations, numerous studies have demonstrated close correlation between both single and dual source CT with CMR for the measurement of ventricular volumes and calculation of cardiac function.

1.4.2 Radiation Dose

Another consideration of functional cardiac CT is the additional radiation dose it requires compared to prospectively triggered axial or high-pitch spiral ("FLASH") mode coronary CTA. Conventional retrospective technique uses full, non-ECG-modulated current delivered throughout the cardiac cycle (Fig. 2). In comparison to a prospectively triggered acquisition, the radiation dose is higher; however,

functional data cannot be extracted using prospective triggering. To limit the dose of radiation delivered to the patient, ECG-modulation can be employed. This is discussed in greater detail in the next section.

2 Technique

2.1 Retrospective Acquisition

In order to extract functional data from a cardiac CT exam, the heart must be imaged in both end-systole and end-diastole. To ensure that the appropriate cardiac phases are imaged, retrospective gating is usually performed. With this technique, a sustained current is generated by the X-ray tube to image throughout the cardiac cycle, during which time the table moves continuously, resulting in a helical acquisition. A low pitch is used in order to image each part of the heart throughout the R–R interval. A simultaneous ECG tracing is obtained corresponding with the image data. This differs from the prospective-triggered axial acquisition in which the tube current is only on during a pre-specified portion of the cardiac cycle, and the table moves in a step-and-shoot fashion. In addition to evaluating cardiac function, retrospective gating is helpful in evaluating patients who have arrhythmias or who are prone to premature or dropped beats because it allows reconstruction of any phase of the cardiac cycle.

ECG-modulation during a retrospectively gated acquisition may be used to reduce the radiation dose. ECG-modulation allows the user to use full current during a certain pre-defined phase of the cardiac cycle, for example between 45–70 % of the R–R interval. During the remaining phases, the tube current is reduced to a pre-specified level (usually 20 % of the maximum, but the level is customizable on some scanner models) (Fig. 3). ECG-modulation with MinDose (Somatom Definition, Siemens Medical Solutions, Germany) reduces this baseline current further to just 4 % (Fig. 4). The reduction in radiation dose depends on the width of the pulse window chosen to deliver the maximum radiation and on the amount of current delivered at baseline. Approximately 40–60 % reduction in radiation dose can be realized using these techniques (Hausleiter et al. 2006, 2007).

2.2 Implication of Scanner Type

Using modern 64-slice MDCT with retrospective gating, a continuous helical scan is obtained over multiple heartbeats with coverage of the entire heart. Due to the retrospective technique, a low pitch is used, creating regions of over-sampling. Newer scanners with expanded z-axis coverage, such as 320-slice MDCT (Aquilion One Dynamic Volume
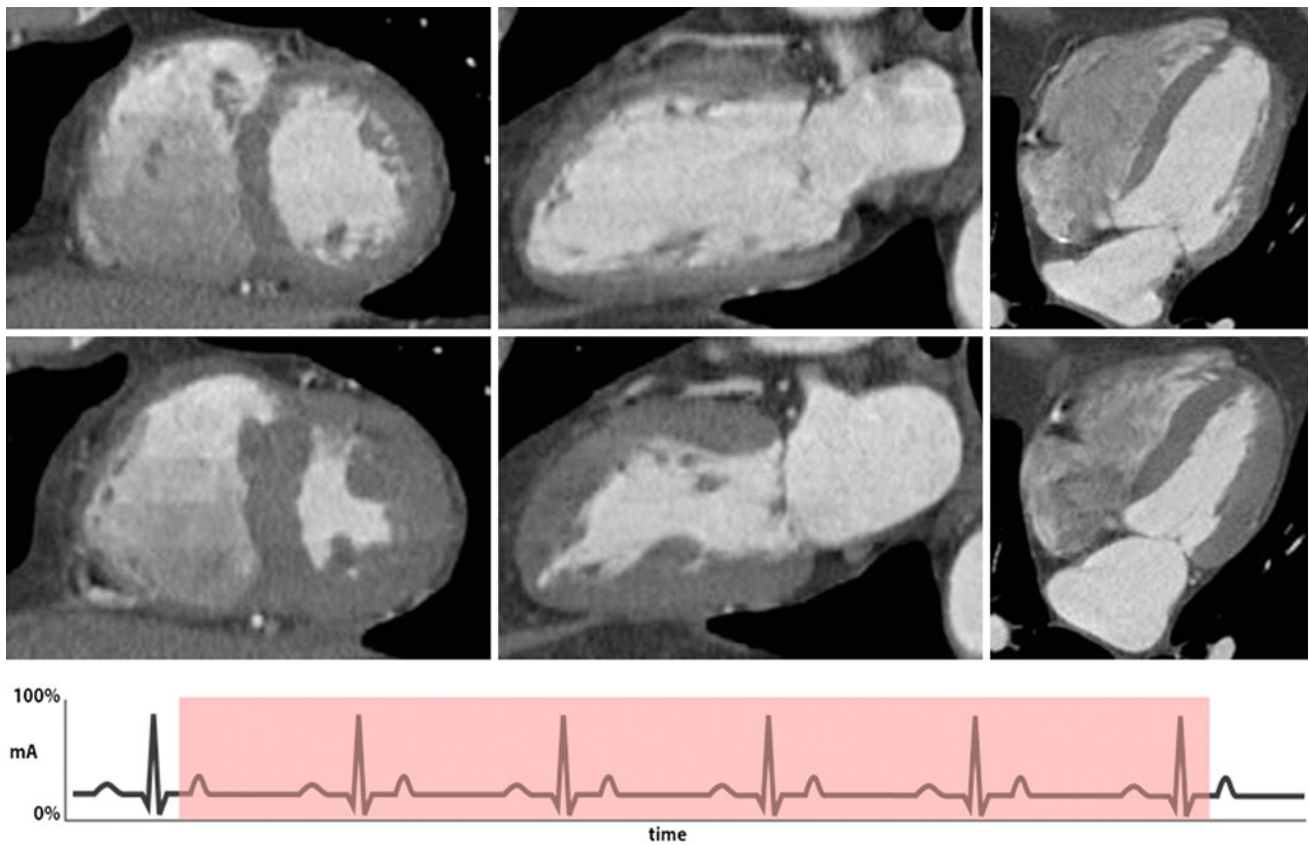
Fig. 2 Example of retrospective gating without tube current modulation. Short-axis (*left*), two-chamber (*middle*), and four-chamber (*right*) views of the heart at end-diastole (*top row*) and end-systole (*bottom row*). With full current delivered at both time points, there is no difference in image quality between the two sets of images. This technique results in a higher radiation dose. An example ECG tracing without tube current modulation is shown demonstrating a sustained acquisition over multiple heartbeats

CT, Toshiba Medical System, Tochigi-ken, Japan), have a detector width of 16 cm allowing a single-heartbeat acquisition. Dual-flash imaging with DSCT during end-systole and end-diastole has been offered as a potential method to obtain functional data without using retrospective gating, with significant reduction in radiation dose. This technique, however, is rarely used in clinical practice and is still under investigation.

2.3 Beta Blockers

Most studies performed for evaluation of the coronary arteries employ the use of beta-blockers to reduce the heart rate for improved image quality. A target heart rate in the high 50 to low 60 s is required for most scanners. While beta-blockade has been shown to improve the diagnostic image quality of the coronary arteries, there is evidence to suggest there are concurrent effects on left ventricular function. A study by Port using echocardiography demonstrated a reduction in ejection fraction in healthy adults after administration of propranolol (Port et al. 1980; Mo et al.

2011). The proposed mechanism is that through negative inotropic action on the heart, ESV increases, thus decreasing the EF. Other studies in healthy patients using cardiac CT for measurement of left ventricular function show similar results, although differences in ESV and EF were modest (Mo et al. 2011).

Studies in patients with heart disease have shown that beta-blockade can produce decreases in measured function, again resulting from increases in ESV (Dell'Italia and Walsh 1989; Jensen et al. 2010). Because most cardiac CTAs performed today are for evaluation for coronary artery disease, the use of beta-blockers for improving image quality usually takes precedence over potential fluctuations in measured LVEF. Scanners with improved temporal resolution (up to 73 ms) have precluded the need for beta-blockade in many patients, particularly when retrospective gating is utilized.

2.4 Contrast Injection

Depending on the cardiac chambers of interest, the injection parameters may require modification from a traditional
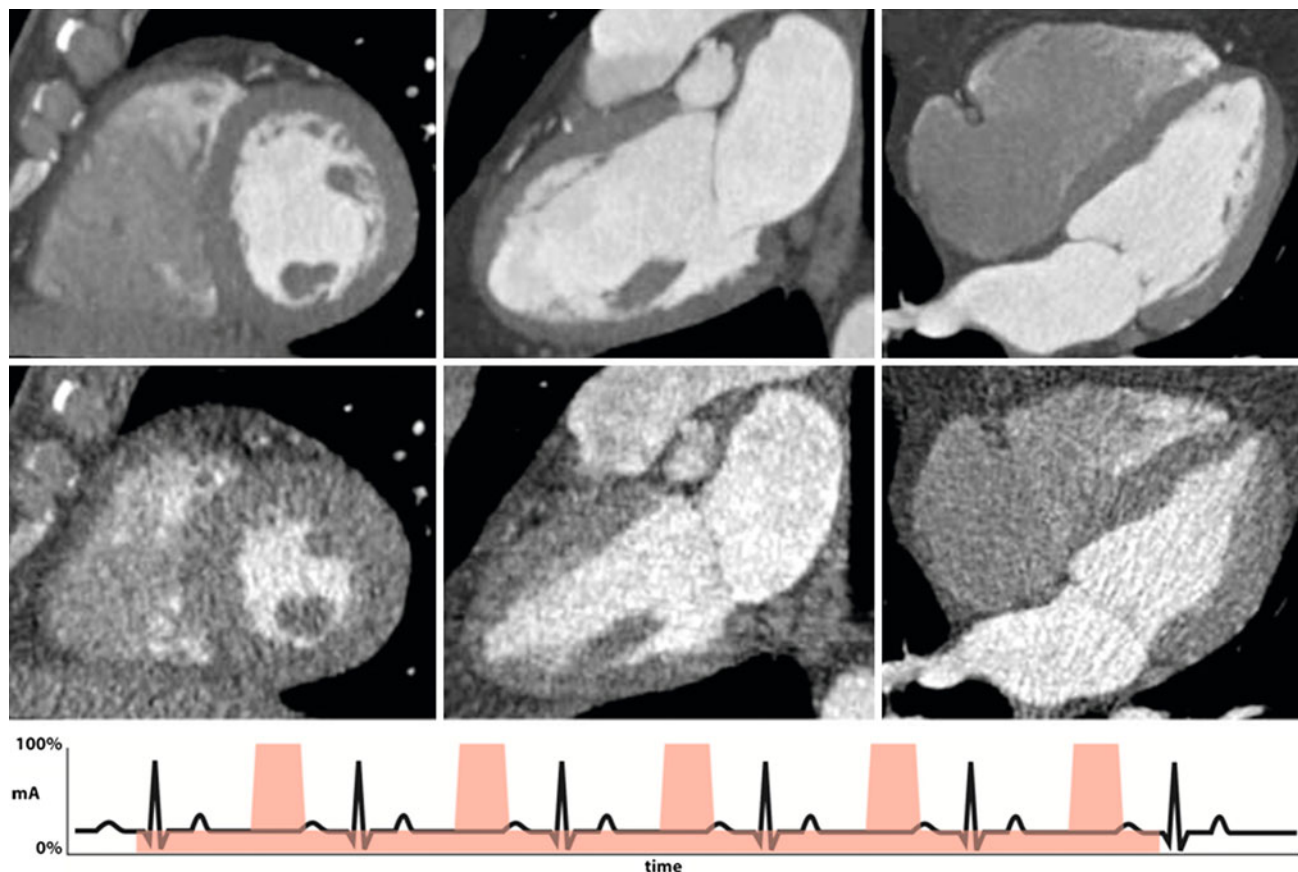
Fig. 3 Example of retrospective gating with tube current modulation. Short-axis (*left*), two-chamber (*middle*), and four-chamber (*right*) views of the heart at end-diastole (*top row*) and end-systole (*bottom row*). Notice the difference in image noise at end-diastole, obtained at full tube current, and end-systole, obtained at 20 % of maximum tube current. Despite the increased image noise at end-systole, images are adequate for delineation of endocardial contours for functional measurement. An example ECG tracing with tube current modulation at 20 % is shown

coronary CTA. Typical coronary CTA employs either bolus tracking or test bolus technique to measure the transit time of the contrast from the site of injection to the ascending aorta. Many institutions utilize a saline chaser after injection of contrast medium. This results in a tighter contrast bolus and reduces streak artifact in the central veins of the thoracic inlet. This technique provides high contrast opacification of the coronary arteries and adequate delineation of the LV endocardium.

In order to achieve adequate, reliable, contrast opacification of both the RV and LV, a multiphasic injection is needed. This involves contrast injection at a normal flow rate (4–7 cc/sec) to opacify the left heart followed by a slower rate (2–4 cc/sec) to opacify the right heart. This is then followed by a saline chaser. An alternative technique is to first inject contrast and follow with a mixture of contrast and saline in a 60:40 or 50:50 ratio. A typical injection may consist of 50 ml of contrast at 6 cc/sec followed by an additional 50 ml of the contrast/saline mixture at 6 cc/sec. Using a multiphasic technique allows contrast opacification of both the left and the right ventricles and reduces the

chance of generating streak artifact from highly concentrated contrast in the SVC, right atrium, or right ventricle (Gao et al. 2012). Lee et al. (2012) analyzed the accuracy of CT in measuring RV function using automated processing software and compared the results to CMR. Low attenuation of the RV blood pool correlated with greater discrepancy with CMR; whereas, when the RV blood pool was greater than 176 HU, measurements were closer to those of CMR, underscoring the importance of proper contrast injection technique.

2.5 Reconstruction Phases

After retrospective scanning, the user has the ability to select the number of phases available for reconstruction. A phase is an interval of the cardiac cycle, usually expressed as a percentage of the RR interval. For example, for reconstruction of cine images, reconstruction of equally spaced phases over the RR interval are obtained, generally in 5 or 10 % increments (yielding 20 or 10 phases,
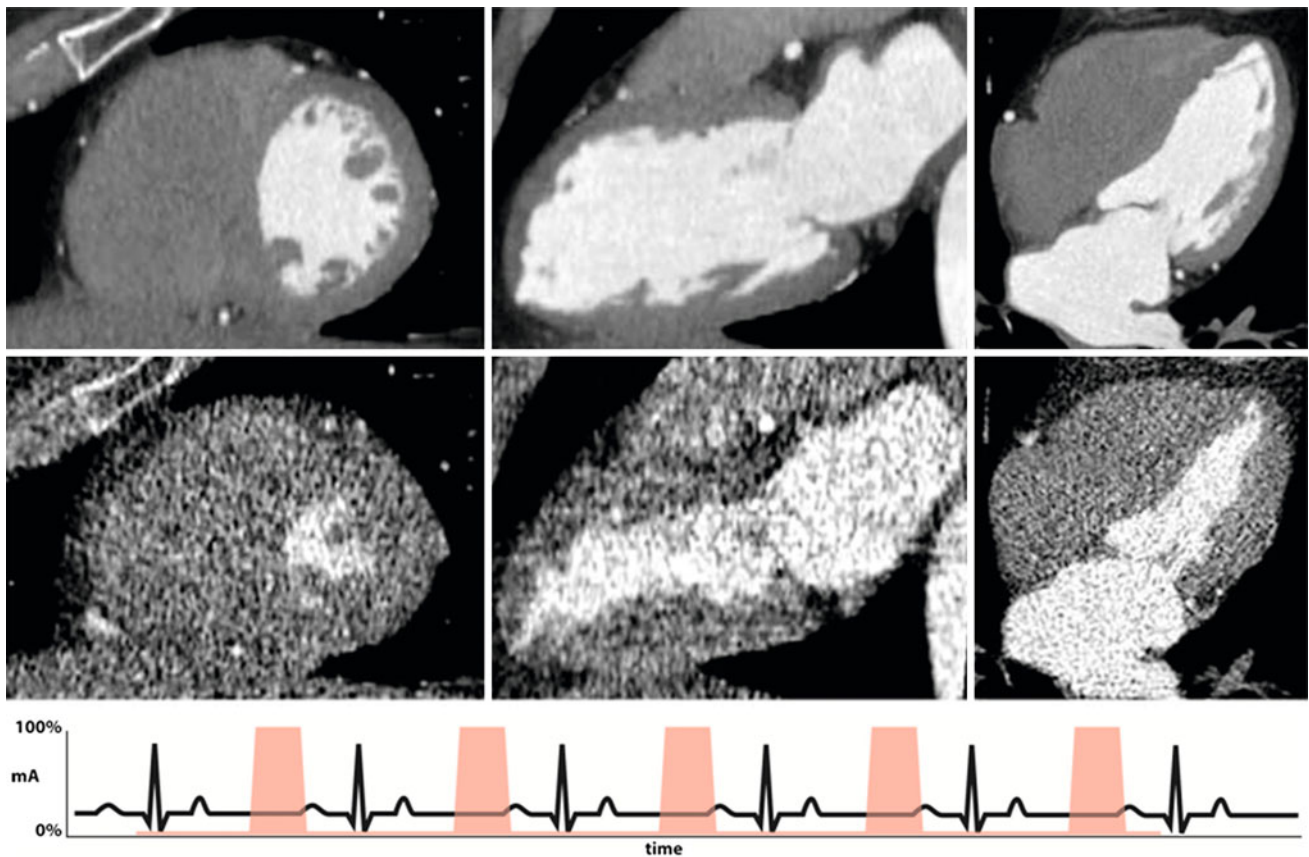
Fig. 4 Example of retrospective gating with tube current modulation down to 4 % of the maximum current. Short-axis (*left*), two-chamber (*middle*), and four-chamber (*right*) views of the heart at end-diastole (*top row*) and end-systole (*bottom row*). There is significant difference in image noise at end-diastole at full tube current and end-systole, respectively). obtained at 4 % of maximum tube current. Despite the increased image noise at end-systole images are quite adequate for delineation of endocardial contours for functional measurement in this relatively thin patient. An example ECG tracing with tube current modulation at 4 % is shown

Increasing the number of phases reconstructed from 10 to 20 doubles the number of images generated for review. A study by Ko et al. (2011) compared 10 and 20 phase reconstruction with respect to cardiac function using a 64-slice scanner. No significant difference in LV volume or EF was observed between the two methods. The increase in the number of phases reconstructed does not change the inherent temporal resolution of the scanner, which is a function of the gantry rotation.

Newer scanners with faster gantry rotation times may be able to take better advantage of more reconstruction intervals. First and second generation dual source CT (DSCT) has the advantage of significantly improved temporal resolution compared to conventional single source CT. Puesken et al. (2008) compared 10 and 20 phase reconstruction using a first generation DSCT. Though use of 20 phases changed the selection of the ES and ED phase in about half of patients, this change resulted in an average 1.9 % change in EF, suggesting that 10 phase reconstruction may be adequate in DSCT as well.

2.6 Post-Processing

One of the major advantages of CT over other modalities is that images are readily acquired as a volumetric dataset. This allows reconstruction of the image in any plane. Modern software packages allow reconstruction of cine images on-the-fly allowing instantaneous visualization of an abnormality in an orthogonal plane. Short axis, 4-chamber, 3-chamber, and 2-chamber views are used to evaluate global function and to evaluate regional wall motion abnormalities. 3-D images of the ventricular blood pool can be obtained with the myocardium subtracted, simulating conventional catheter ventriculography.

2.7 Semi-automatic Versus Automatic Versus Manual

There are multiple methods available to quantify right and left ventricular volumes ranging from time-intensive

manual techniques to fully automated software packages. All techniques rely on measurements in end-diastole and end-systole.

The area-length method is a technique borrowed from echocardiography and can be used in calculating left ventricular volume with CT. As the name implies, this technique relies on the measurement of the area and length of the left ventricle. The area is calculated in either the vertical or horizontal long axis plane. The length is measured as the distance from the mitral valve plane to the apex. Using the following formula, left ventricular volume is then calculated.

$$\text{Volume} = \frac{8}{3} \times \frac{A^2}{\pi \times L}$$

This formula uses geometric assumptions about the left ventricle, specifically assuming an ellipsoid shape. A variation of the area-length method is the *biplane* area-length method which uses both the vertical and horizontal long axes to calculate the volume.

Simpson's method is commonly used in calculating ventricular volume in CMR and can be used to calculate both left and right ventricular volume. In contrast to the area-length method, Simpson's method does not rely on assumptions about ventricular shape. Using this technique, contours are drawn around the endocardial border in end-systole and end-diastole in the short-axis plane. Each contour represents a volume determined by the slice thickness and gap or overlap. The contours are summed using the following formula where A is the cross-sectional area and S is the slice thickness plus gap, or slice thickness minus overlap.

$$\text{Volume} = \sum A_N \times S$$

Studies comparing area-length method and Simpson's method have shown close agreement between the two, even in patients with regional wall motion abnormalities, although there is slight overestimation of EDV, ESV, and SV using the area-length method (Lessick et al. 2008).

Semi-automated and fully automated software packages are available from multiple vendors. These use a threshold-based segmentation that detects the difference in attenuation between the ventricular chamber and the myocardium; thus, adequate opacification of the blood pool is required. The main advantage of these techniques is the significant time savings over manual processing. A byproduct of semi-automated and fully automated segmentation is that once the mitral valve plane is defined, all available phases can be segmented, allowing time-volume curves to be drawn. Studies comparing manual, semi-automated, and fully automated software have shown close correlation of ventricular volumes using these methods with significant reduction in processing time and good interobserver variability (Greupner et al. 2011; Juergens et al. 2008; Plumhans et al. 2009).

A caveat of the threshold-based methods is that papillary muscles are excluded from the blood pool. This results in systematic underestimation of EDV and ESV as well as overestimation of EF compared to CMR. However, when the same software tools and measurement methods are used for analysis of both the CT and MR, close agreement between the two modalities is observed (de Jonge et al. 2011).

The threshold method is also susceptible to errors from high-attenuation material. For example, streak artifact from dense contrast in the central veins or right heart can lead to errors in contour detection. Pacemaker leads can cause the software to include the right atrial or ventricular chambers in the LV blood pool. Ventricular septal defects can cause similar errors owing to a continuous, unbroken column of contrast (Juergens et al. 2008; van Ooijen et al. 2012).

2.8   Calculation of Values

Once EDV and ESV are acquired, simple subtraction of the values yields the stroke volume (SV); that is, the amount of blood ejected from the ventricle with each beat. Importantly, the SV calculated using this method includes blood flow in any direction, not exclusively flow through the ventricular outflow tract. Regurgitant flow through the mitral or tricuspid valve and ventricular septal defects will be included in this value. As an internal check, and in the absence of valvular regurgitation or shunting, the stroke volume in the RV and LV should be the same.

$$\text{SV(ml)} = \text{EDV} - \text{ESV}$$

Cardiac output can then be obtained by multiplying the SV by the heart rate.

$$\text{CO(ml/min)} = \text{SV} \times \text{HR}$$

The ejection fraction is calculated by determining the percentage of blood exiting the ventricle using the EDV as the baseline.

$$\text{EF(\%)} = \frac{\text{SV}}{\text{EDV}} \times 100$$

Normalization of these values to the body surface area (BSA) is helpful to stratify results.

3 Left Ventricle

3.1 Normal Values

Numerous studies have defined the normal values of left ventricular volume using CMR and echocardiography. Because of differences in temporal resolution, image quality, and measurement technique, values obtained with other modalities should not be translated to CT (Lin et al. 2008). Values normalized to BSA are given below.

Normal values for the left ventricle using MDCT				
Parameter	Men		Women	
	Mean	SD	Mean	SD
ESV (ml)	48.56	16.13	29.58	11.1
EDV (ml)	143.58	28.11	102.14	12.61
ESVI (ml/m^2)	24.48	8.51	17.63	6.66
EDVI (ml/m^2)	72.35	15.09	60.86	13.31
EF (%)	66.9	7.3	71.6	7.9

ESV end-systolic volume, *EDV* end-diastolic volume, *ESVI* end-systolic volume index, *EDVI* end-diastolic volume index, *EF* ejection fraction (Nevsky et al. 2011)

3.2 Comparison with Echo, MR

The combination of excellent temporal resolution and good spatial resolution make CMR the current gold standard for the evaluation of left ventricular function. Numerous studies have evaluated measurements of left ventricular function using CCT compared with CMR. A meta-analysis of 8–16 slice MDCT compared to CMR demonstrated close correlation of ESV, EDV, and LVEF. The use of multi-segmental reconstruction algorithms showed improvement in correlation, likely owing to increased temporal resolution allowed by these techniques (van der Vleuten et al. 2006).

Current scanner technologies, including 64-, 128-, 256-, 320-slice single source CT, and dual source CT (64 and 128 slice), have also shown excellent correlation with CMR even without the use of multi-segmental reconstruction algorithms due to improvement in temporal resolution.

3.3 Wall Motion Abnormalities

3.3.1 Introduction

Abnormal wall motion can be divided into regional abnormalities affecting parts of the myocardium and global abnormalities affecting an entire chamber. Regional wall motion abnormalities at rest are usually attributed to rest ischemia or myocardial infarction and can be mapped to a coronary territory; global abnormalities are usually due to either severe multivessel disease or non-ischemic cardiomyopathy.

3.3.2 Segmental Assessment

CT data are acquired in an axial plane in relation to the body axis. Volumetric data is then reconstructed in planes analogous to those used in echocardiography and nuclear medicine, i.e., long and short axes with respect to the ventricular long axis. For diagnostic consistency among imaging modalities and to allow correlation between coronary anatomy and wall segments, the traditional AHA 17-segment model is used in CT when describing regional wall motion abnormalities. Using this model, the basal and mid-ventricular LV levels are divided into six segments, the apical level is divided into four segments, and the apex constitutes a final segment.

Regional wall motion abnormalities are usually assessed qualitatively based on cine images. Wall motion abnormalities can be described as *akinetic* in the absence of systolic thickening, *hypokinetic* when wall motion is subnormal, or *dyskinetic* when there is paradoxical motion compared to other regions (i.e., outward bulging during systole, lack of coordination). Quantitative measurements can also be made based on the amount of wall thickening compared to adjacent normal myocardium. There is significant regional variation within the same patient, and more so between patients, but estimates for normal myocardial thickness are 6–8 mm at end-diastole and 10–14 mm at end-systole for normal systolic thickening of approximately 5 mm (Juergens and Fischbach 2006).

3.3.3 Global Assessment

Global function or dysfunction refers to both the qualitative assessment of myocardial movement and wall thickening as well as the quantitative measurement of volume and

CT versus MRI	n	CT scanner	EDV			ESV			EF		
			r	Bias (ml)	SD (ml)	r	Bias (ml)	SD (ml)	r	Bias (%)	SD (%)
Dual source CT											
Takx et al. (2012)	20	DSCT[a]	0.89	−5.1	21.6	0.95	−5.7	14.7	0.87	5.1	7.6
Bastarrika et al. (2008)	12	DSCT	0.70	16.6	18.6	0.39	4.9	6.9	0.64	−0.3	3.2
Brodoefel et al. (2007)	20	DSCT	0.98	−2.2		0.99	−1.4		0.95	0.7	

(continued)

CT versus MRI	n	CT scanner	EDV			ESV			EF		
			r	Bias (ml)	SD (ml)	r	Bias (ml)	SD (ml)	r	Bias (%)	SD (%)
Busch et al. (2008)	15	DSCT	0.81	3.7	25.4	0.79	−2.6	17.3	0.64	3.8	9.4
Jensen et al. (2010)	32	DSCT	0.87	−1.3	17.7	0.92	1.0	8.3	0.83	−1.0	4.5
Lunders	30	DSCT	0.96	−0.3	18.2	0.98	1.1	7.8	0.97	−1.1	7.8
van der Vleuten et al. (2009)	34	DSCT	0.96	11.0	54.8	0.97	3.5	31.9	0.90	0.4	4.5
64 SLICE CT											
Akram et al. (2009)	20	64	0.80	0.6	21.4	0.86	−2.3	8.5	0.92	1.6	3.4
Annuar et al. (2008)	32	64	0.98	−8.8	12.5	0.98	−6.3	9.8	0.92	−2.3	6.7
Guo et al. (2009)	51	64	0.93	5.7	27.8	0.92	0.8	17.5	0.89	1.3	5.7
Maffei et al. (2012)	79	64	0.59	3.3	25.8	0.76	2.6	35.1	0.73	0.6	21.1
Sarwar et al. (2009)	21	64	0.91			0.94			0.90		
Schlosser et al. (2007)	21	64		−19.9	20.3		−13.4	10.3		3.9	7.5
Wu et al. (2008a)	41	64	0.96			0.98			0.95		
Wu et al. (2008b)	63	64	0.98	−0.6	15.2	0.99	1.1	10.6	0.97	−0.2	−4.2
4-16 SLICE CT											
Belge et al. (2006)	40	16	0.92			0.95			0.95		
Dewey et al. (2006)	88	16	0.87	−6.2	20.7	0.92	−5.2	12.9	0.91	2.1	5.2
Fischbach et al. (2007)	30	16	0.96	−16.8	19.4	0.94	6.9	10.2	0.83	−2.5	4.2
Grude et al. (2003)	30	4	0.80	14.2	17.3	0.89	17.8	10.3	0.85	−8.5	4.7
Halliburton	15	4	0.26	−35.2		0.62	−22.4		0.30	−1.6	
Heuschmid et al. (2005)	31	16	0.86	13.2	21.9	0.91	8.7	15.9	0.87	1.4	5.2
Juergens et al. (2004)	30	4	0.93	0.4	11.8	0.94	0.2	7.2	0.89	0.3	0.5
Koch et al. (2004) SAX	19	16	0.98	−3.2		0.98	−7.3		0.95	3.0	
Koch et al. (2004) 3D TH			0.96	−4.8		0.98	−4.6		0.91	0.3	
Mahnken et al. (2005)	21	16	0.99	−1.0	1.9	0.99	−0.4	1.6	0.99	−0.1	1.0
Mahnken et al. (2003) (std)	15	4		−7.5	3.4		−1.7	4.4		0.8	3.3
Mahnken et al. (2003) (mult)				−0.3	1.0		−0.3	1.0		0.5	2.1
Matthias	37	4	0.80	14.1	17.3	0.89	17.8	10.3	0.85	−0.9	4.7
Raman et al. (2006)	26	16	0.97	−2.7	7.8	0.97	−1.0	7.4	0.97	0.3	3.6
Salm et al. (2006)	25	16							0.86	−1.5	8.6
Schlosser et al. (2007) (std)	18	16		−17.2	13.1		−9.1	10.9		2.6	7.3
Schlosser et al. (2007) (auto)				−20.3	15.7		−9.2	13.9		1.0	9.0
Sugeng et al. (2006)	31	16	0.98	26.0	21.4	0.97	19.0	25.5	0.92	−2.8	6.6
Yamamuro et al. (2005)	50	8	0.97	−0.4	15.2	0.99	1.1	8.6	0.96	−1.2	4.6

EDV end-diastolic volume, *ESV* end-systolic volume, *EF* ejection fraction, *SD* standard deviation

[a] Indicates second generation DSCT

function. Qualitatively, normal myocardium should demonstrate brisk systolic contraction and wall thickening. Hypofunctioning myocardium can be uniform or it can demonstrate regional variation with some segments demonstrating worse function compared to others. Global function can also be described as hyperdynamic, commonly seen in patients with hypertrophic cardiomyopathy. Assessment of global LV function carries important prognostic implications. Data from the Coronary Artery Surgery Study (CASS) registry showed that in patients with cardiac ischemia, the ejection fraction was more closely associated with adverse outcomes than the number of diseased coronary vessels; as the EF decreased below 45 %, the risk of death increased in a linear fashion. (Mock et al. 1982).

3.4 Disease Entities of the LV

3.4.1 Chronic Ischemia

Segments of myocardium that are chronically ischemic but still metabolically active may demonstrate reduced function in the form of segmental hypokinesis. This is referred to as hibernating myocardium. Hibernating myocardium is clinically important to differentiate from nonviable myocardium because revascularization by angioplasty, stenting, or grafting may restore function to these segments. PET and CMR are now the most commonly used tools to evaluate for viable, hibernating myocardium although CT is beginning to play a larger role in this realm. This topic is discussed in further detail in subsequent chapters.

3.4.2 Acute Infarcts

Within a few minutes after an acute myocardial infarct, there is development of a regional wall motion abnormality in the distribution of a coronary territory, usually demonstrated by an akinetic segment. Depending on the transmurality of the infarct and remaining functioning myocardium, regional wall motion abnormalities may improve over time as stunned but still viable myocardium regains function (Mahias-Narvarte 1987). Sarwar et al. (2009) examined 64-slice CT compared to CMR for evaluating global and regional left ventricular function specifically in patients recently reperfused after acute myocardial infarction. Quantification of LV volumes and EF by CT was shown to correlate well with values obtained by CMR. CCT demonstrated 89 % sensitivity and 92 % specificity in detecting abnormal segments (on a per-segment basis) using CMR as the standard.

In the setting of acute chest pain, functional evaluation of the left ventricle with CT has been shown to add incremental value to the assessment of the coronary arteries by CTA. In the Rule Out Myocardial Infarction Using Computer Assisted Tomography (ROMICAT) trials, patients with chest pain, initial negative troponin, non-ischemic EKG, but clinical suspicion for acute coronary syndrome (ACS) were arranged to have a coronary CTA with retrospective gating. The diagnostic accuracy of CTA for the detection of ACS was 77 % with coronary evaluation alone; the addition of a resting regional LV function increased the diagnostic accuracy to 87 %. LV wall motion abnormalities can also help to direct attention to lesions that are too small to resolve by CTA such as side branches or small vessels (Seneviratne et al. 2010).

3.4.3 Chronic Infarcts

The appearance of a chronic infarct can be variable by CT depending on the territory and severity of the infarct. Transmural infarcts will demonstrate focal wall thinning in a coronary distribution with regional akinesis or dyskinesis. (Figure 5) Fatty metaplasia or calcification can be seen in place of normal myocardium.

In cases of transmural infarction, a left ventricular aneurysm may form. In the strict definition, an aneurysm is a focal contour deformity with wall thinning that moves paradoxically (i.e. dyskinetic) in relation to the rest of the myocardium. Most aneurysms involve the apical anterior wall resulting from a transmural LAD infarct. Inferior basal wall infarcts are second most common location. In cases of non-transmural infarction, residual functioning or hibernating myocardium prevents aneurysm formation but may result in focal akinesis or hypokinesis (Glower and Ei 2003).

3.4.4 Non-ischemic Cardiomyopathies

Non-ischemic cardiomyopathies are intrinsic diseases of the heart muscle and can be divided into primary and secondary diseases. Some secondary causes include alcohol, chemotherapy, sarcoid, and genetic diseases. The World Health Organization and the International Society and Federation of Cardiology Task Force divides primary cardiomyopathies into 5 categories: dilated cardiomyopathy, hypertrophic cardiomyopathy, restrictive cardiomyopathy, arrhythmogenic right ventricular dysplasia, and unclassified disease. These diseases are characterized primarily by either normal function or global hypokinesis, although regional variation may be evident in some cases.

Functional imaging in patients with dilated cardiomyopathy typically shows an enlarged left ventricle with global LV hypokinesis. The right ventricle can be involved in some cases. Not infrequently, the apex is completely akinetic. (Figure 6) Hypertrophic cardiomyopathy is characterized by poor base-to-apex shortening and obliteration of the cavity at the LV apex. The calculated ejection fraction is usually supranormal. In patients with restrictive cardiomyopathy, LV contraction is preserved but relaxation in diastole is impaired. Common causes of restrictive disease

Fig. 5 Two-chamber (*left*) and short-axis (*right*) views of the *left* ventricle in end-diastole (*top row*) and end-systole (*bottom row*). This patient had a remote history of LAD infarct. Note the focal anterior wall thinning with only minimal increase in wall thickness on systolic images, consistent with nontransmural remote infarct
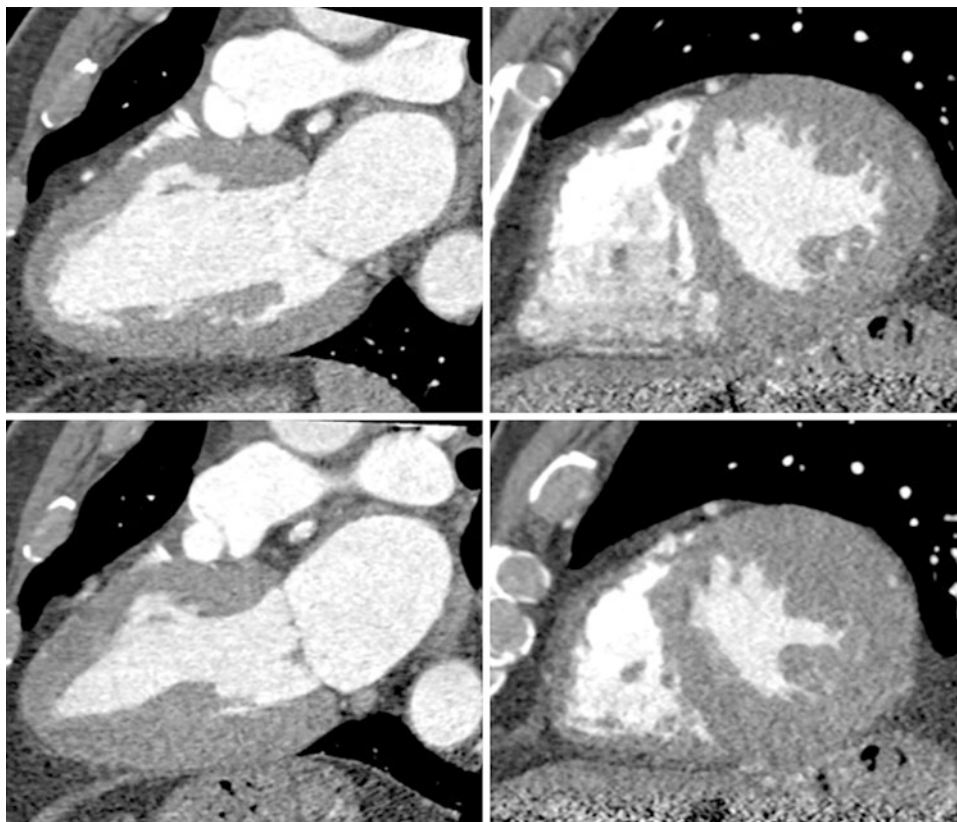
include amyloid, sarcoid, hemochromatosis, and glycogen storage diseases.

Tako-tsubo cardiomyopathy is an uncommon entity that can mimic an acute coronary syndrome. Patients usually describe a recent emotional stressor; thus, the alternative term of "broken-heart syndrome" has also been used. Functional imaging demonstrates dyskinesis of the mid and apical segments causing a ballooning of the LV in systole. Basilar function is usually preserved. Function returns to normal within a few days.

3.4.5 Heart Transplant

Patients with heart transplant typically present a unique problem for cardiac CT owing to a high resting heart rate and body mass index, as well as altered cardiac anatomy (Ferencik et al. 2007). Improvements in immunosuppressive therapies have increased survival to approximately 50 % at 10 years and 30 % at 15 years (Taylor et al. 2008). Longer survival has uncovered new challenges, such as cardiac allograph vasculopathy. CCTA can offer a one-stop-shop solution for follow up of these patients by evaluating both the coronary vessels and cardiac function. Studies using both MDCT and DSCT have shown accurate assessment of left ventricular function compared to CMR (Mastrobuoni et al. 2011; Bastarrika et al. 2008). The use of DSCT with improved temporal resolution is especially helpful in these patients due to the high resting heart rate.

4 Right Ventricle

4.1 Normal Values

Normal values for the right ventricle using MDCT	
ESD (mm)	29.6 ± 5.3
EDD (mm)	37.0 ± 5.7
EDV (ml)	174.9 ± 48.0
ESV (ml)	82.1 ± 29.2
EF (%)	57.9 ± 8.0

(Lin et al. 2008)

4.2 Indications

Imaging of the RV poses special challenges because of its unique shape and the presence of irregular trabeculations. Echocardiography is particularly problematic because the RV is mostly retrosternal in position and acoustic windows are limited. Thus, cross-sectional imaging plays an important role in patients with right heart disease. Assessment of right ventricular function carries important prognostic information in patients with acute diseases, such as acute respiratory distress syndrome and pulmonary embolism
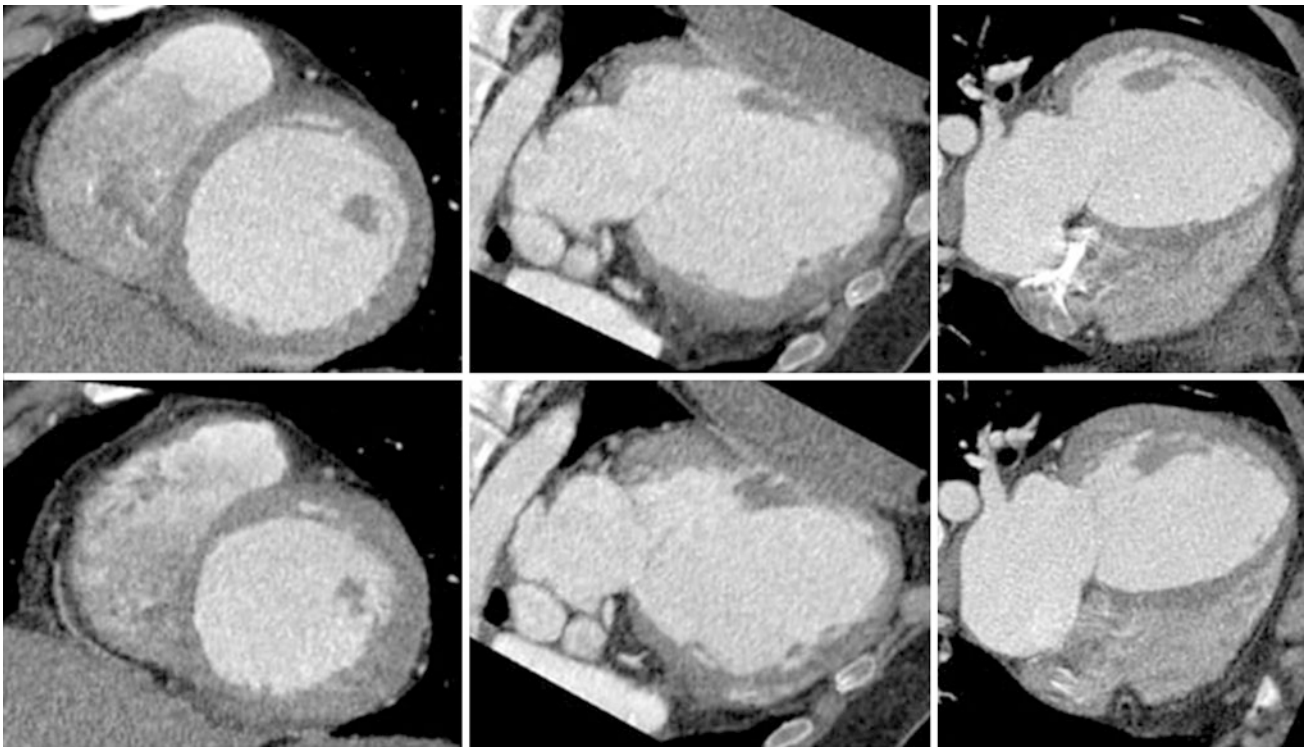
Fig. 6 Short-axis (*left*), two-chamber (*middle*), and four-chamber (*right*) views of the *left* ventricle in end-diastole (*top row*) and end-systole (*bottom row*) in a patient with dilated cardiomyopathy. The *left* ventricle is markedly enlarged. Note the lack of significant movement or wall thickening on systolic images (*bottom*) indicating globally reduced systolic function. The EF in this patient was 15 %

(PE). For example, in patients with acute PE, right ventricular dysfunction is associated with higher rates of intubation, ICU admission, and death. Rapid selection of patients with right ventricular dysfunction can help assess those patients who need catheter-directed thrombolysis or surgical embolectomy (Kang et al. 2011).

Measurement of RV volume and function also carries important prognostic significance in chronic lung diseases resulting in cor pulmonale. In patients with COPD, increased RV end-diastolic volume and decreased RV function are strongly associated with decreased survival (Burgess et al. 2002). A multitude of diffuse lung diseases are associated with cor pulmonale including interstitial lung disease, vascular disorders causing pulmonary hypertension, and sleep-related breathing disorders.

Liver disease is an established cause of increased right heart volumes. This can occur through portopulmonary hypertension, hepatopulmonary syndrome, or as a result of TIPS therapy (Dupont et al. 2011). Finally, many congenital heart diseases, such as tetralogy of Fallot, transposition of the great vessels, arrhythmogenic right ventricular dysplasia/cardiomyopathy, and double outlet right ventricle, affect the RV (Savino et al. 2007). In these patients, serial measurement of RV function can be an important part of surveillance.

4.3 Pulmonary Embolism

4.3.1 RV:LV Ratio

Small, subsegmental pulmonary emboli do not usually induce RV dysfunction because of the compensatory mechanisms of the pulmonary arterial system. However, as the clot burden in the pulmonary arteries increases, signs of RV strain can begin to show; a 30–40 % obstruction of the pulmonary arterial tree can result in modest increases in right ventricular pressure. With continued increase in pulmonary arterial obstruction, right ventricular failure can develop causing increases in right and left atrial volume (Fishman et al. 2008). Many of these functional changes in the right ventricle can be gleaned without retrospective imaging or even cardiac gating.

The relative volume of the RV can be estimated by comparing the short-axis dimension with the LV. This measurement should be obtained perpendicular to the long axis of the heart, ideally using a 4-chamber reconstruction, measuring from the right ventricular free wall to the septum. An RV:LV ratio greater than 1 is a sign of increased right ventricular volume (Fig. 7).

This sign can be quickly assessed in patients being evaluated for pulmonary embolism as an indicator of right ventricular volume overload and right heart strain. Often, a
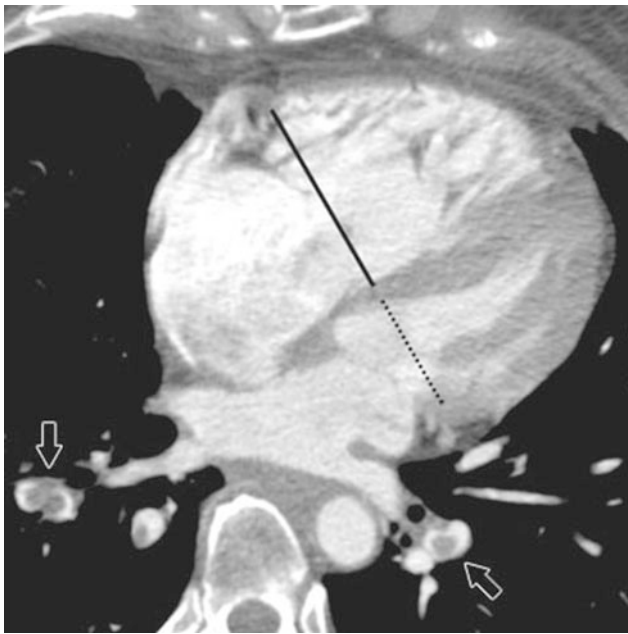
Fig. 7 Four-chamber view of the heart demonstrates bowing of the interventricular septum with convexity into the *left* ventricle. The maximal dimension of the RV (*solid line*) was much greater than the LV (*dotted line*). The RV:LV ratio in this patient was 1.6. Notice segmental pulmonary emboli in the *right* and *left* lower lobe pulmonary arteries (*arrows*)

crude measurement can be made on axial images, roughly approximating a 4-chamber view. However, measurement in the 4-chamber view is more sensitive for the stratification of patients with severe disease. A study by Quiroz et al. demonstrated that measurement of the RV:LV ratio in the 4-chamber view increased the receiver operating curve for the prediction of adverse events including the need for resuscitation, mechanical ventilation, pressors, thrombolysis, or surgical embolectomy (Quiroz et al. 2004).

4.3.2 Septal Bowing

Static images of the heart may show straightening or concave bowing of the interventricular septum into the left ventricular cavity. This can be a sign of increased right ventricular volume, pressure, or both. Gated images can help to distinguish between these two entities. Increased right ventricular pressure will demonstrate bowing of the septum throughout the cardiac cycle; whereas, in volume overload, the septal bowing often normalizes during systole. The presence of increased right ventricular wall thickness suggests chronic pressure overload.

4.3.3 Systemic Vein Diameter

As right ventricular failure progresses, excess volume is translated to the right atrium and systemic veins. Measurements of the SVC, azygous vein, and coronary sinus are

usable surrogates for right ventricular dysfunction in patients with PE. These measurements can be done relatively quickly in the axial plane and have been shown to correlate with elevated PA pressures measured by echocardiography. For example, coronary sinus dimension of 16 mm or greater was shown to correlate with peak systolic PA pressures of greater than 30 mmHg compared to a median diameter of 10 mm in patients with pressures less than 30 mmHg. A reasonable cutoff for the SVC is 25 mm in diameter and 10 mm in diameter for the azygos vein (Staskiewicz et al. 2010).

4.4 ARVD/C

Arrhythmogenic right ventricular dysplasia is a cardiomyopathy in which there is replacement of myocardium in the RV by fibrofatty tissue. Patients may be asymptomatic, but may also present with arrhythmias and sudden cardiac death; biventricular heart failure can be seen in late stages of the disease. Partially in an attempt to detect earlier disease, revisions to the original 1994 International Task Force criteria have been proposed, increasing the emphasis on imaging, specifically with echocardiography, CMR, and angiography (Marcus et al. 2010). Major criteria by angiography include RV akinesia, dyskinesia, or aneurysm. Evaluation of suspected ARVD has been included as an appropriate indication for functional CCT in the 2010 ACCF appropriateness criteria (Taylor et al. 2010).

4.5 Congenital Heart Disease

Serial measurement of RV volume and function may be important in following patients with some congenital heart disease. Common congenital anomalies like atrial or ventricular septal defects and partial anomalous pulmonary venous return represent an over-circulation phenomenon with chronic left-to-right shunts. Depending on the severity of shunting, these patients may demonstrate RV dilatation as well as pulmonary artery enlargement. Patients with repaired tetralogy of Fallot often have incompetent pulmonic valves and a dilated right ventricle. In these patients, serial quantification of RV function is important because it affects the timing of pulmonic valve replacement.

5 Left Atrium

5.1 Indication

Left atrial volume and functional measurement is recognized as a marker for the evaluation of patients with atrial

fibrillation, left heart failure with normal ejection fraction, mitral valve disease, and stroke. An enlarged left atrium is a risk factor for recurrent atrial fibrillation after pulmonary vein isolation (Abecasis et al. 2009; Helms et al. 2009). Cross-sectional imaging of the left atrium with MDCT or CMR can be used for treatment planning for left atrial ablation or pulmonary vein isolation. Measurement of the left atrial volume is more accurate and correlates more closely with the clinical course (Tsang et al. 2006).

5.2 Normal Values

Normal values for left atrium using MDCT in women and men		
Indexed measurement	Women	Men
EDV/BSA (ml/m^2)	40 ± 9 (37–43)	41 ± 10 (38–44)
ESV/BSA (ml/m^2)	18 ± 6 (16–20)	22 ± 6 (20–24)
SV/BSA (ml/m^2)	22 ± 4 (21–23)	19 ± 6 (17–21)
EF (%)	55 ± 8 (52–57)	46 ± 8 (43–48)
Diameter/BSA (mm/m^2)	18 ± 4 (17–19)	17 ± 2 (16–18)

EDV end-diastolic volume, *ESV* end-systolic volume, *SV* stroke volume, *BSA* body surface area
Normal values in units indicated ± SD (95 % CI)
(Stojanovska et al. 2011)

5.3 Comparison with Other Techniques

Two-dimensional echocardiography is the most commonly used method to assess left atrial size due to availability and portability. In some cases, measurement of the left atrium by echocardiography can be limited. As is the case in imaging of the left ventricle, image quality is degraded in patients with a large body habitus. Because of the posterior position of the left atrium, lateral resolution can be reduced, limiting accurate delineation of the endocardial contour (Avelar et al. 2010). Additionally, foreshortening of the maximal left atrial plane can cause underestimation of the volume. These variables may be responsible for the increased interobserver variability of echocardiography in assessing left atrial volume compared to CT or MRI (Avelar et al. 2010). Though there is good correlation with CT and MR, many studies have demonstrated systematic underestimation of left atrial volume by echocardiography (Rodevan et al. 1999; Avelar et al. 2010; Christiaens et al. 2009; Kircher et al. 1991). In contrast, volumetric and functional measurements made by CT show close correlation with MRI, although studies have shown a slight trend for overestimating LA volumes and underestimating LA ejection fraction (Wen et al. 2010).

5.4 Technique

Assessment of left atrial volume and function can usually be done using the same data set used to acquire the left ventricle. Retrospective technique with EKG-gated tube current modulation permits adequate delineation of the LA contour while allowing significant reduction in radiation dose.

Volumetric analysis can be obtained manually using Simpson's method. Both semi-automated and fully automated software packages are available as well.

Diastole can be divided into the isovolumetric relaxation phase and the filling phase. The main component of the filling phase is rapid filling, which accounts for 70–80 % of LV blood volume. A short diastases period follows, contributing another 5 % of blood volume. Finally, atrial systole contributes the remaining 15–25 % of LV blood volume before the start of ventricular systole (Braunwald 2008).

5.5 Heart Failure with Preserved Ejection Fraction

Impaired relaxation of the LV results in characteristic changes in LA volume and function. Compared to patients of hypertension and left ventricular hypertrophy, patients with HFpEF have increased LA volume and reduced LA ejection fraction, and these markers have been shown to be a reliable method to differentiate the two conditions (Melenovsky et al. 2007).

6 Summary

Improvements in CT technology have advanced significantly such that accurate and reliable determination of global and regional cardiac function can be made with little additional cost. Advanced post-processing software has significantly reduced the time in generating data. At the same time, hardware improvements have substantially reduced radiation dose. Functional and volume measurement of the LV, RV, and LA have shown excellent correlation with the gold standard CMR.

References

Abecasis J, Dourado R, Ferreira A, Saraiva C (2009) Left atrial volume calculated by multi-detector computed tomography may predict successful pulmonary vein isolation in catheter ablation of atrial fibrillation. Eurospace 11:1289–1294

Akram K, Anderson HD, Voros S (2009) Quantification of left ventricular parameters obtained by automated software for 64-slice multidetector computed tomography and comparison with magnetic resonance imaging. Cardiovasc Intervent Radiol 32(6):1154–1160

Annuar BR, Liew CK, Chin SP, Ong TK, Seyfarth MT, Chan WL, Fong YY, Ang CK, Lin N, Liew HB, Sim KH (2008) Assessment of global and regional left ventricular function using 64-slice multislice computed tomography and 2D echocardiography: a comparison with cardiac magnetic resonance. Eur J Radiol 65(1):112–119

Avelar E et al (2010) Comparison of the accuracy of multidetector computed tomography versus two-dimensional echocardiography to measure left atrial volume. Am J Cardiol 106(1):104–109

Bastarrika G, Arraiza M, De Cecco CN, Mastrobuoni S, Ubilla M, Rabago G (2008) Quantification of left ventricular function and mass in heart transplant recipients using dual-source CT and MRI: initial clinical experience. Eur Radiol 18(9):1784–1790

Bavelaar-Croon CD et al (2000) Left ventricular function: correlation of quantitative gated SPECT and MR imaging over a wide range of values. Radiology 217(2):572–575

Belge B, Coche E, Pasquet A, Vanoverschelde JL, Gerber BL (2006) Accurate estimation of global and regional cardiac function by retrospectively gated multidetector row computed tomography: comparison with cine magnetic resonance imaging. Eur Radiol 16(7):1424–1433

Braunwald E (2008) Braunwald's heart disease: a textbook of cardiovascular medicine. In: Peter L, Robert B, Douglas M Douglas Z. Saunders (eds) Elsevier, Philadelphia

Brodoefel H, Kramer U, Reimann A, Burgstahler C, Schroeder S, Kopp A, Heuschmid M (2007) Dual-source CT with improved temporal resolution in assessment of left ventricular function: a pilot study. Am J Roentgenol 189(5):1064–1070

Burgess MI, Mogulkoc N, Bright-Thomas RJ, Bishop P, Egan JJ, Ray SG (2002) Comparison of echocardiographic markers of right ventricular function in determining prognosis in chronic pulmonary disease. J Am Soc Echocardiogr 15:633–639

Busch S, Johnson TR, Wintersperger BJ, Minaifar N, Bhargava A, Rist C, Reiser MF, Becker C, Nikolaou K (2008) Quantitative assessment of left ventricular function with dual-source CT in comparison to cardiac magnetic resonance imaging: initial findings. Eur Radiol 18(3):570–575

Christiaens L et al (2009) A new method for measurement of LA volumes using 64-slice spiral CT: comparison with 2DE techniques. Int J Cardiol 131:217–224

de Geus-Oei LF et al (2011) Scintigraphic techniques for early detection of cancer treatment-induced cardiotoxicity. J Nucl Med 52(4):560–571

de Jonge GJ et al (2011) Semi-automatic measurement of left ventricular function on dual source computed tomography using five different software tools in comparison with magnetic resonance imaging. Eur J Radiol 80(3):755–766

Dell'Italia LJ, Walsh RA (1989) Effect of intravenous metoprolol on left ventricular performance in Q-wave acute myocardial infarction. Am J Cardiol 63(3):166–171

Dewey M, Müller M, Teige F, Schnapauff D, Schink T, Hamm B, Lembcke A (2006) Multisegment and halfscan reconstruction of 16-slice computed tomography for assessment of regional and global left ventricular myocardial function. Invest Radiol 41(4):400–409

Dupont MVM, Dragean CA, Coche EE (2011) Right ventricle function assessment by MDCT. Am J Roentgenol 196(1):77–86

Ferencik M et al (2007) Analysis of cardiac dimensions, mass and function in heart transplant recipients using 64-slice multi-detector computed tomography. J Heart Lung Transplant 26(5):478–484

Fischbach R, Juergens KU, Ozgun M, Maintz D, Grude M, Seifarth H, Heindel W, Wichter T (2007) Assessment of regional left ventricular function with multidetector-row computed tomography versus magnetic resonance imaging. Eur Radiol 17(4):1009–1017

Fishman AP, Elias JA, Fishman JA, Grippi MA, Senior RM, Pack AI (2008) Fishman's pulmonary diseases and disorders, 4th edn. McGraw Hill Medical, New York

Gao Y, Du X, Liang L, Cao L, Yang Q, Li K (2012) Evaluation of right ventricular function by 64-row CT in patients with chronic obstructive pulmonary disease and cor pulmonale. Eur J Radiol 81(2):345–353

Glower D Di, Lowe J Ei (2003) Left ventricular aneurysm. In: Cohn LH, Edmunds LH Jr (ed) Cardiac surgery in the adult. McGraw-Hill, New York, pp 771–788

Greupner J, Zimmermann E, Hamm B, Dewey M (2011) Automatic versus semi-automatic global cardiac function assessment using 64-row computed tomography. Br J Radiol 34(5):367–374

Grude M, Juergens KU, Wichter T, Paul M, Fallenberg EM, Muller JG, Heindel W, Breithardt G, Fischbach R (2003) Evaluation of global left ventricular myocardial function with electrocardiogram-gated multidetector computed tomography: comparison with magnetic resonance imaging. Invest Radiol 38(10):653–661

Guo YK, Yang ZG, Ning G, Rao L, Dong L, Pen Y, Zhang TM, Wu Y, Zhang XC, Wang QL (2009) Sixty-four-slice multidetector computed tomography for preoperative evaluation of left ventricular function and mass in patients with mitral regurgitation: comparison with magnetic resonance imaging and echocardiography. Eur Radiol 19(9):2107–2116

Hammermeister KE, DeRouen TA, Dodge HT (1979) Variables predictive of survival in patients with coronary disease. Selection by univariate and multivariate analyses from the clinical, electro-cardiographic, exercise, arteriographic, and quantitative angio-graphic evaluations. Circulation 59(3):421–430

Hausleiter J et al (2006) Radiation dose estimates from cardiac multislice computed tomography in daily practice. Circulation 113:1305–1310

Hausleiter J et al (2007) A new algorithm for ECG-based tube current modulation (MinDose) reduces radiation dose estimates in cardiac dual source CT angiography. Circulation 116:II_575

Helms AS et al (2009) Relation of left atrial volume from three-dimensional computed tomography to atrial fibrillation recurrence following ablation. Am J Cardiol 103:989–993

Jensen CJ, Jochims M, Hunold P, Forsting M, Barkhausen J, Sabin GV, Bruder O, Schlosser T (2010) Assessment of left ventricular function and mass in dual-source computed tomography coronary angiography: Influence of beta-blockers on left ventricular function: comparison to magnetic resonance imaging. Eur J Radiol 74(3):484–491

Juergens KU, Grude M, Maintz D, Fallenberg EM, Wichter T, Heindel W, Fischbach R (2004) Multi-detector row CT of left ventricular function with dedicated analysis software versus MR imaging: initial experience. Radiology 230(2):403–410

Juergens KU, Roman F (2006) Left ventricular function studied with MDCT. Eur Radiol 16:342–357

Juergens KU et al (2008) Automated threshold-based 3D segmentation versus short-axis planimetry for assessment of global left ventricular function with dual-source MDCT. Am J Roentgenology 190(2):308–314

Kang DK et al (2011) CT Signs of right ventricular dysfunction. JACC: Cardiovasc Imaging 4(8):841–849

Kircher B et al (1991) Left atrial volume determination by biplane two-dimensional echocardiography: validation by cine CT. Am Heart J 121:864–871

Ko YJ, Kim SS, Park WJ, Jeong JO, Ko SM (2011) Comparison of global left ventricular function using 20 phases with 10-phase reconstructions in multidetector-row computed tomography. Int J Cardiovasc Imaging 28(3):603–611

Koch K, Oellig F, Kunz P, Bender P, Oberholzer K, Mildenberger P, Hake U, Kreitner KF, Thelen M (2004) Assessment of global and regional left ventricular function with a 16-slice spiral-CT using two different software tools for quantitative functional analysis and qualitative evaluation of wall motion changes in comparison with magnetic resonance imaging. Rofo 176(12):1786–1793

Lee H, Kim SY, Gebregziabher M, Hanna EL, Schoepf J (2012) Impact of ventricular contrast medium attenuation on the accuracy of left and right ventricular function analysis at cardiac multi detector-row CT compared with cardiac MRI. Acad Radiol 19:(4):395–405

Lessick J, Ghersin E, Abadi S, Yalonetsky S (2008) Accuracy of the long-axis area-length method for the measurement of left ventricular volumes and ejection fraction using multidetector computed tomograph. Can J Cardiol 24(9):685–689

Lin FY et al (2008) Cardiac chamber volumes, function, and mass as determined by 64-multidetector row computed tomography: mean values among healthy adults free of hypertension and obesity. JACC Cardiovasc Imaging 1(6):782–786

Helena M-N, Adams KF, Willis PW (1987) Evolution of regional left ventricular wall motion abnormalities in acute Q and non-Q wave myocardial infarction. Am Heart J 113(6):1369–1375

Heuschmid M, Rothfuss J, Schröder S, Küttner A, Fenchel M, Stauder N, Mahnken AH, Burgstahler C, Miller S, Claussen CD, Kopp AF (2005) Left ventricular functional parameters: comparison of 16-slice spiral CT with MRI. Rofo 177(1):60–66

Maffei E, Messalli G, Martini C, Nieman K, Catalano O, Rossi A, Seitun S, Guaricci AI, Tedeschi C, Mollet NR, Cademartiri F (2012) Left and right ventricle assessment with Cardiac CT: validation study vs. Cardiac MR. Eur Radiol 22(5):1041–1049

Mahnken AH, Spuentrup E, Niethammer M, Buecker A, Boese J, Wildberger JE, Flohr T, Sinha AM, Krombach GA, Günther RW (2003) Quantitative and qualitative assessment of left ventricular volume with ECG-gated multislice spiral CT: value of different image reconstruction algorithms in comparison to MRI. Acta Radiol 44(6):604–611

Mahnken AH, Koos R, Katoh M, Spuentrup E, Busch P, Wildberger JE, Kühl HP, Günther RW (2005) Sixteen-slice spiral CT versus MR imaging for the assessment of left ventricular function in acute myocardial infarction. Eur Radiol 15(4):714–720

Marcus FI et al (2010) Diagnosis of arrhythmogenic right ventricular cardiomyopathy/dysplasia - proposed modification of the task force criteria. Circulation 121:1533–1541

Mastrobuoni S et al (2011) Allograft morphology and function in heart transplant recipients surviving more than 15 years by magnetic resonance imaging and dual-source computed tomography. Eur J Cardiothorac Surg 40(1):e62–e66

Melenovsky V, Borlaug B, Rosen B et al (2007) Cardiovascular features of heart failure with preserved ejection fraction versus non-failing hypertensive left ventricular hypertrophy in the urban Baltimore community. J Am Coll Cardiol 49:198–207

Mo YH, Jaw FS, Wang YC, Jeng CM, Peng SF (2011) Effects of propranolol on the left ventricular volume of normal subjects during CT coronary angiography. Korean J Radiol 12(3):319

Mock MB et al (1982) Survival of medically treated patients in the coronary artery surgery study (CASS) registry. Circulation 66:562–568

Nevsky G, Jacobs JE, Lim RP, Donnino R, Babb JS, Srichai MB (2011) Sex-specific normalized reference values of heart and great vessel dimensions in cardiac CT angiograph. Am J Roentgenol 196:788–794

Plumhans C et al (2009) Comparison of manual, semi- and fully automated heart segmentation for assessing global left ventricular function in multidetector computed tomography. Invest Radiol 44(8):476–482

Port S, Cobb FR, Jones RH (1980) Effects of propranolol on left ventricular function in normal men. Circulation 61(2):358–366

Puesken M et al (2008) Global left-ventricular function assessment using dual-source multidetector CT: effect of improved temporal resolution on ventricular volume measurement. Eur Radiol 18(10):2087–2094

Quiroz R et al (2004) Right ventricular enlargement on chest computed tomography: prognostic role in acute pulmonary embolism. Circulation 109(20):2401–2404

Raman SV, Shah M, McCarthy B, Garcia A, Ferketich AK (2006) Multi-detector row cardiac computed tomography accurately quantifies right and left ventricular size and function compared with cardiac magnetic resonance. Am Heart J 151(3):736–744

Rodevan O, Bjornerheim R, Ljosland M, Maehle J, Smith HJ, Ihlen H (1999) Left atrial volumes assessed by three- and two-dimensional echocardiography compared to MRI estimates. Int J Card Imaging 15:397–410

Salm LP, Schuijf JD, de Roos A, Lamb HJ, Vliegen HW, Jukema JW, Joemai R, van der Wall EE, Bax JJ (2006) Global and regional left ventricular function assessment with 16-detector row CT: comparison with echocardiography and cardiovascular magnetic resonance. Eur J Echocardiogr 7(4):308–314

Sarwar A et al (2009) Evaluating global and regional left ventricular function in patients with reperfused acute myocardial infarction by 64-slice multidetector CT: a comparison to magnetic resonance imaging. J Cardiovasc Comput Tomogr 3(3):170–177

Savino G et al (2007) CT of cardiac function. J Thoracic Imaging 22(1):86–100

Schlosser T, Mohrs OK, Magedanz A, Voigtlander T, Schmermund A, Barkhausen J (2007) Assessment of left ventricular function and mass in patients undergoing computed tomography (CT) coronary angiography using 64-detector-row CT: comparison to magnetic resonance imaging. Acta Radiologica 48:30–35

Seneviratne SK et al (2010) Incremental diagnostic value of regional left ventricular function over coronary assessment by cardiac computed tomography for the detection of acute coronary syndrome in patients with acute chest pain: from the ROMICAT trial. Circ Cardiovasc Imaging 3(4):375–383

Setser RM, Fischer SE, Lorenz CH (2000) Quantification of left ventricular function with magnetic resonance images acquired in real time. J Magn Reson Imaging 12:430–438

Slart R et al (2004) Comparison of gated PET with MRI for evaluation of left ventricular function in patients with coronary artery disease. J Nucl Med 45(2):176–182

Staskiewicz G et al (2010) Widening of coronary sinus in CT pulmonary angiography indicates right ventricular dysfunction in patients with acute pulmonary embolism. Eur Radiol 20:1615–1620

Stojanovska J et al (2011) Reference normal absolute and indexed values from ECG-gated MDCT: left atrial volume, function, and diameter. Am J Roentgenology 197(3):631–637

Stollfuss JC et al (1998) Regional myocardial wall thickening and global ejection fraction in patients with low angiographic left ventricular ejection fraction assessed by visual and quantitative resting ECG-gated 99mTc-tetrofosmin single-photon emission tomography and magnetic resonance imaging. Eur J Nucl Med 25(5):522–530

Sugeng L, Mor-Avi V, Weinert L, Niel J, Ebner C, Steringer-Mascherbauer R, Schmidt F, Galuschky C, Schummers G, Lang RM, Nesser HJ (2006) Quantitative assessment of left ventricular size and function: side-by-side comparison of real-time three-dimensional echocardiography and computed tomography with magnetic resonance reference. Circulation 114(7):654–661

Takx RA, Moscariello A, Schoepf UJ, Barraza JM Jr, Nance JW Jr, Bastarrika G, Das M, Meyer M, Wildberger JE, Schoenberg SO,

Fink C, Henzler T (2012) Quantification of left and right ventricular function and myocardial mass: comparison of low-radiation dose 2nd generation dual-source CT and cardiac MRI. Eur J Radiol 81(4):e598–e604

Taylor DO et al (2008) Registry of the International Society for Heart and Lung Transplantation: twenty-fifth official adult heart transplant report—2008. J Heart Lung Transplant 27(9):943–956

Taylor AJ et al (2010) ACCF/SCCT/ACR/AHA/ASE/ASNC/SCAI/SCMR 2010 appropriate use criteria for cardiac computed tomography. J Am Coll Cardiol 56(22):1864–1894

Tsang TS et al (2006) Prediction of cardiovascular outcomes with left atrial size: is volume superior to area or diameter? J Am Coll Cardiol 47:1018–1023

van der Vleuten PA et al (2006) Quantification of global left ventricular function: comparison of multidetector computed tomography and magnetic resonance imaging. a meta-analysis and review of the current literature. Acta Radiol 47(10):1049–1057

van der Vleuten PA, de Jonge GJ, Lubbers DD, Tio RA, Willems TP, Oudkerk M, Zijlstra F (2009) Evaluation of global left ventricular function assessment by dual-source computed tomography compared with MRI. Eur Radiol 19(2):271-277

van Ooijen PM, de Jonge GJ, Oudkerk M (2012) Informatics in radiology: postprocessing pitfalls in using CT for automatic and semiautomatic determination of global left ventricular function. Radiographics 32(2):589–599

Wen Z, Zhang Z, Yu W, Fan Z, Du J, Lv B (2010) Assessing the left atrial phasic volume and function with dual-source CT: comparison with 3T MRI. Int J Cardiovasc Imaging 26:88–92

Wu YW, Tadamura E, Kanao S, Yamamuro M, Okayama S, Ozasa N, Toma M, Kimura T, Kita T, Marui A, Komeda M, Togashi K (2008a) Left ventricular functional analysis using 64-slice multi-detector row computed tomography: comparison with left ventriculography and cardiovascular magnetic resonance. Cardiology 109(2):135–142

Wu YW, Tadamura E, Yamamuro M, Kanao S, Okayama S, Ozasa N, Toma M, Kimura T, Komeda M, Togashi K (2008b) Estimation of global and regional cardiac function using 64-slice computed tomography: a comparison study with echocardiography, gated-SPECT and cardiovascular magnetic resonance. Int J Cardiol 128(1):69–76

Yamamuro M, Tadamura E, Kubo S, Toyoda H, Nishina T, Ohba M, Hosokawa R, Kimura T, Tamaki N, Komeda M, Kita T, Konishi J (2005) Cardiac functional analysis with multi-detector row CT and segmental reconstruction algorithm: comparison with echocardiography, SPECT, and MR imaging.Radiology 234(2):381–390